Experimental investigation of abnormal transverse flow enhancement of math xmlns="http://www.w3.org/1998/Math/MathML">mi>α/mi> /math> particles in heavy-ion collisions

Y. Huang, W. Lin, H. Zheng, R. Wada, A. Bonasera, Z. Chen, J. Han, R. Han, M. Huang, K. Hagel, T. Keutgen, X. Liu, Y. G. Ma, C. W. Ma, Z. Majka, G. Qu, L. Qin, P. Ren, G. Tian, J. Wang, Z. Yang, and J. B. Natowitz

Phys. Rev. C **104**, 044611 — Published 12 October 2021

DOI: 10.1103/PhysRevC.104.044611

Experimental investigation on abnormal transverse flow enhancement of α particles in heavy-ion collisions

Y. Huang[a], W. Lin[a], H. Zheng[b], R. Wada[c,d], A. Bonasera[c,e], Z. Chen[f], J. Han[a], R. Han[f], M. Huang[g], K. Hagel[c], T. Keutgen[h], X. Liu[a,*], Y. G. Ma[i,j], C. W. Ma[d], Z. Majka[k], G. Qu[a], L. Qin[a], P. Ren[a], G. Tian[f], J. Wang[l], Z. Yang[m], J. B. Natowitz[c]

[a] Key Laboratory of Radiation Physics and Technology of the Ministry of Education, Chengdu 610064, China
[b] School of Physics and Information Technology, Shaanxi Normal University, Xi'an 710119, China
[c] Cyclotron Institute, Texas A&M University, College Station, Texas 77843
[d] School of Physics, Henan Normal University, Xinxiang 453007, China
[e] Laboratori Nazionali del Sud, INFN,via Santa Sofia, 62, 95123 Catania, Italy
[f] Institute of Modern Physics, Chinese Academy of Sciences, Lanzhou 730000, China
[g] College of Physics and Electronics information, Inner Mongolia University for Nationalities, Tongliao, 028000, China
[h] FNRS and IPN, Université Catholique de Louvain, B-1348 Louvain-Neuve, Belgium
[i] Key Laboratory of Nuclear Physics and Ion-Beam Application (MOE), Institute of Modern Physics, Fudan University, Shanghai 200433, China
[j] Shanghai Institute of Applied Physics, Chinese Academy of Sciences, Shanghai 201800, China
[k] Jagiellonian University, Krakow, Poland
[l] School of Science, Huzhou University, Huzhou 313000, China
[m] Science and Technology on Reactor System Design Technology Laboratory, Nuclear Power Institute of China, Chengdu 610213, China

Abstract

The mass dependence of the transverse flow for Z=1-5 fragments from the collisions of ^{40}Ar+^{27}Al, ^{40}Ar+^{48}Ti and ^{40}Ar+^{58}Ni at 47 MeV/nucleon is investigated experimentally in this article. The transverse flow values are determined using the in-plane components of the fragment transverse momenta, where three conventional methods, i.e., the kinetic flow tensor method, the transverse momentum analysis method, and the azimuthal correlation method, are applied to reconstruct the reaction plane in an event-by-event basis. It is demonstrated from the comparison of the present experimental mass dependent flow measurements and the model simulations using an improved antisymmetrized molecular dynamics model, that the experimentally observed abnormal α transverse flow enhancement is closely related to the reaction plane reconstruction procedure in the flow extraction. We further investigate the physical existence of the abnormal α flow behavior using a two-particle azimuthal correlation method, which allows to provide the relative flow magnitude information with an identification of fragment charge number without the knowledge of the reaction plane differing from the three conventional methods. It is found that the relative flow magnitudes deduced from the two-particle azimuthal correlation functions with an identification of Z, with the correction for the recoil effect imposed by the momentum conservation, show a monotonically increasing trend as function of fragment charge number, with no exception of the α flow enhancement. These results, in addition to those from the improved antisymmetrized molecular dynamics model simulations, definitely provide experimental evidences for the inexistence of the abnormal α flow behavior in the heavy-ion collisions at the present incident energy region in nature.

1. Introduction

The study of transverse flow is of great importance in nuclear physics, as it helps to constrain key parameters in nuclear physics, such as the nuclear equation of state (EOS), effective nucleon-nucleon (NN) interaction and the in-medium NN cross sections etc, and elucidate the mechanism of reaction dynamics, comparing the experimental results to dynamical calculations [1, 2, 3, 4, 5, 6]. The transverse flow, also known as directed flow, is usually considered as a one-body observable [7]. In the heavy-ion collisions at intermediate energies, fragments with $Z \geq 2$ are copiously produced and they also carry abundant information on the characteristic feature of the reaction dynamics similar to free neutrons and protons. To gain insights into the transverse flow for the fragments, efforts have been made to measure the flow exclusively with the identification of mass (or charge) numbers of fragments in the heavy-ion collisions [8, 9]. As a consequence, a significant dependence of transverse flow on fragment mass in a wide mass range has been observed, that is, the measured flow increases smoothly as the fragment mass increases, except for an abnormal flow enhancement for α particles [8, 9].

Recently, we studied the mass dependence of the transverse flow in the ^{40}Ca+^{40}Ca collisions at 35 MeV/nucleon, and observed a similar abnormal α flow enhancement [10]. This abnormal α flow behavior could not be explained by the interplay between the thermal and collective motions under a momentum conservation. We further examined possible origins for the observed abnormal α flow behavior in the aspects of reaction dynamics, sequential decay process, experimental detection and off-line data analyses [11], within the framework of

*Email address: liuxingquan@scu.edu.cn

an improved antisymmetrized molecular dynamics model with the specific consideration of the Fermi motion in the *NN* collisions (AMD-FM) [12, 13]. In that work, it was found that the abnormal α flow behavior is closely related to the imperfect reconstruction of the reaction plane in the flow extraction [11].

The aim of this article is to experimentally investigate the correlation of the abnormal α flow behavior and the reaction plane reconstruction, and to further clarify whether the experimentally observed abnormal α flow behavior exists physically. In this work, the transverse flow values for the fragments with different masses are first extracted using the in-plane components of the fragment transverse momenta from the collisions of ^{40}Ar+^{27}Al, ^{40}Ar+^{48}Ti and ^{40}Ar+^{58}Ni at 47 MeV/nucleon. The kinetic flow tensor method [14], the transverse momentum analysis method [15, 16], and the azimuthal correlation method [17] are applied for the reaction plane reconstruction in an event-by-event basis, respectively. The sensitivity of the transverse flow dependence on the fragment mass to the selection of the reaction plane reconstruction method is carefully examined in the three reaction systems. The physical existence of the experimentally observed abnormal α flow behavior is discussed based on the present experimental flow measurements and the AMD-FM simulations. To date, some powerful techniques, i.e., the two-particle azimuthal correlation method of Wang *et al.* [18], the transverse momentum analysis technique of Danielewicz *et al.* [19] etc, have been developed to deduce the flow information without reconstructing the reaction plane. Here, we choose the two-particle azimuthal correlation method to further pursue the question of the physical existence of abnormal α flow behavior. The article is organized as follows. In Sec. 2, the experiment and data analysis are briefly described, in which the three reaction plane reconstruction methods are specified. In Sec. 3, the flow results experimentally deduced using the reconstructed reaction planes and using the reaction plane-free two-particle azimuthal correlation method, as well as those from the AMD-FM simulations, are presented and discussed. Summary and prospectives are given in Sec. 4.

2. Experiment and data analysis

a. Experimental setup and particle identification

The experiment was performed at the Cyclotron Institute, Texas A&M University. ^{40}Ar beams delivered from the K500 superconducting cyclotron impinged on the ^{27}Al, ^{48}Ti and ^{58}Ni targets at an incident energy 47 MeV/nucleon. The reaction products were detected using a 4π array, NIMROD-ISiS (Neutron Ion Multidetector for Reaction Oriented Dynamics with the Indiana Silicon Sphere) [20], consisting of a charged particle array combined with the Texas A&M Neutron Ball [21] outside. The charged particle array consisted of 14 concentric detector rings covering 3.6° to 167° in the laboratory frame. Twelve to twenty-four charged particle detector modules were set in each detector ring. In each of the forward rings at $\theta_{lab} \leq 45°$, two special modules (referred as super telescopes) were set having two Si detectors (150 and 500 μm) in front of a CsI(Tl) detector (2.8-10.0 cm long). The other modules in the forward and backward rings had one Si detector (either 150, 300 or 500 μm) followed by a CsI(Tl) detector (referred as single telescope). The pulse shape discrimination method for the fast and slow components of the CsI light output provided the isotopic identification of the light charged particles with $Z \leq 2$ (LCPs), and the energy loss versus remaining energy in Si-CsI and Si-Si provided the identification of the intermediate mass fragments with $Z > 2$ (IMFs). Isotopic resolution of the IMFs was achieved up to Z=8, and elemental identification was achieved for all detected fragments, for the super telescopes. The IMFs detected in the single telescopes were typically identified up to Z=14 in atomic number. The neutron ball surrounding the charged particle array was also used to determine the neutron multiplicity in an event-by-event basis during the experiment, although the neutron data were not used in the present work. Details about the experimental setup, and basic observables obtained from the experiment such as energy spectra and particle multiplicities have been presented in Refs. [22, 23].

b. Event characterization

The events measured are first subjected to an off-line event filter, requiring that the detected $Z_{tot} \geq 50\% \times Z_{sys}$, where Z_{tot} and Z_{sys} are the total detected charge number in each event and the charge number of the reaction system, respectively. The collision centrality of the remaining events is evaluated utilizing the charged particle multiplicity detected in the forward hemisphere in the center-of-mass frame, taking the advantage of the good isotopic and elemental resolutions in the forward rings. Following Refs. [24, 25], the relationship between the charged particle multiplicity N_{ch} and the reduced impact parameter b/b_{max} can be written as

$$(b/b_{max})^2 = \int_{N_{ch}}^{\infty} \frac{dP(N_{ch})}{dN_{ch}} \cdot dN_{ch}, \qquad (1)$$

where b and b_{max} are the impact parameter and the maximum impact parameter, respectively. b_{max} is normally taken as the summation of the radii of the projectile and the target nuclei, where $R_{proj(targ)} = 1.2A^{1/3}_{proj(targ)}$. $dP(N_{ch})/dN_{ch}$ is the normalized probability distribution for a given N_{ch} with $\int_1^{\infty} \frac{dP(N_{ch})}{dN_{ch}} \cdot dN_{ch} \equiv 1$. Figure 1 shows (a) the normalized N_{ch} distributions and (b) b/b_{max} versus N_{ch} obtained from Eq. (1), for the three reaction systems, ^{40}Ar+^{27}Al, ^{40}Ar+^{48}Ti and ^{40}Ar+^{58}Ni from the left to the right, respectively. Since the transverse flow appears strongest in the semi-central collisions [2, 26, 27], the events with b/b_{max}=0.3-0.7 are selected for the present flow analysis. The corresponding N_{ch} intervals for the event selection are mapped out from the panels (b) of Fig. 1 to be 4-7, 5-8 and 6-9 for ^{40}Ar+^{27}Al, ^{40}Ar+^{48}Ti and ^{40}Ar+^{58}Ni, respectively.

c. Reaction plane reconstruction

The reaction plane is defined geometrically by the momentum vector of the projectile and the impact parameter vector. Four methods have been proposed for reconstructing

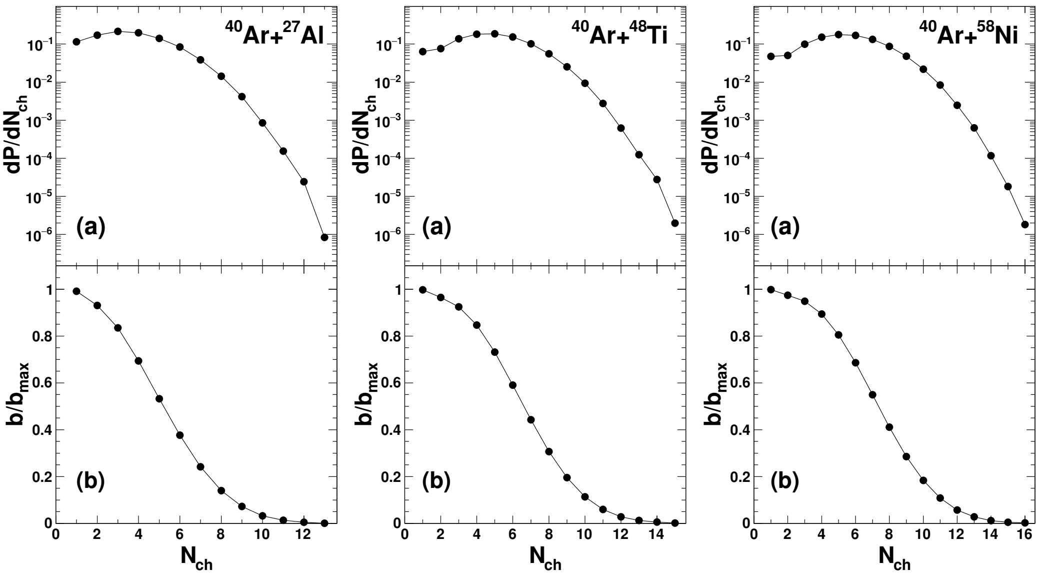

Figure 1: (a) Normalized charged particle multiplicity N_{ch} distributions. (b) Reduced impact parameter b/b_{max} versus N_{ch} evaluated using Eq. (1). Left, middle and right subfigures are from the systems of ^{40}Ar+^{27}Al, ^{40}Ar+^{48}Ti and ^{40}Ar+^{58}Ni, respectively.

the reaction plane in the literature, i.e., kinetic flow tensor (KFT) method [14], transverse momentum analysis (TMA) method [15, 16], azimuthal correlation (AC) method [17], and projectile-like fragment plane (PFP) method [28, 29].

Historically, the KFT method was the first proposed. For each event the 3×3 kinetic-flow tensor in the Cartesian coordinate is defined as

$$F_{ij} = \sum_{\nu} \omega(\nu) P_i(\nu) P_j(\nu) \quad i, j = x, y, z, \tag{2}$$

with $P_i(\nu)$ being the components of the momentum vector of the νth particle in the event. $\omega(\nu)$ is the scalar weight factor and often taken to be $1/m(\nu)$ with $m(\nu)$ being the mass of the particle. The summation runs over all particles in the entire event. In heavy-ion collisions, F_{ij} represents a volume with a cigar-like shape in general. The tensor is symmetric in the way defined and hence determined by six independent values. Diagonalization allows the determination of the three eigenvalues, λ_i (i=1, 2 and 3). The angle between the eigenvector $\vec{e_1}$ associated with the largest eigenvalue λ_1 and the beam axis defines the flow angle, and therefore, the reaction plane is defined as the plane constraining $\vec{e_1}$ and the beam axis. The positive direction of the in-plane x-axis is defined by the direction of the $\vec{e_1}$ component perpendicular to the beam axis.

Danielewicz *et al.* later proposed the TMA method to reconstruct the reaction plane [15]. In the standard TMA method, a vector $\vec{Q}$, defining the reaction plane together with the beam direction, is constructed from the transverse momenta of particles,

$$\vec{Q} = \sum_{\nu} \omega(\nu) \vec{P}_t(\nu), \tag{3}$$

where $\vec{P}_t(\nu)$ is the transverse momentum of the νth particle. The scalar weight factor $\omega(\nu)$ is positive for particles emitted at the forward hemisphere in the center-of-mass frame and negative otherwise. Typical values for $|\omega(\nu)|$ are taken to be 1.0 or $m(\nu)$, the mass of the νth particle. In this work, the former, $|\omega(\nu)| = 1.0$, is adopted. The summation in the equation is taken over the particles in each event. The $\vec{Q}$ direction defines the positive direction of the in-plane x-axis. Since the transverse momentum for a given particle, namely particle of interest (POI), is used both for the reaction plane reconstruction and for the projection, autocorrelation is involved [16], leading to the POI being assessed to be emitted closer to the reconstructed reaction plane. The autocorrelation effect can be amplified by the loss of information due to the incomplete detection of the particles in one event. To avoid the autocorrelation, the POI is removed from the summation of Eq. (3) in practice [16], so that different reaction planes are assigned for different particles in a given event. The reconstructed reaction plane after taking into account the autocorrelation effect is referred to "one reaction plane per particle" elsewhere [17]. It should be emphasized that the KFT method does not consider the autocorrelation effect in its original form, since it was designed to fit the distribution of promptly emitted particles using a spheroid, and the angle determined by the eigenvector of the long axis $\vec{e_1}$ and the beam axis can be treated to be the absolute flow angle itself. Later in the flow study of Cussol *et al.* [9], the KFT method was improved with specific consideration for the autocorrelation effect by removing the POI from the summation in Eq. (2). Following Ref. [9], the one plane per particle prescription is also used in the reaction plane reconstruction with the KFT method in the present work.

In the AC method [17], the deviation of the particles from the reaction plane in the momentum space D^2 for a given event is introduced using a parameter k, which is taken as the slope of the projection line of the reaction plane onto the $x - y$ plane in the coordinate. D^2 is defined by the summation of the perpen-

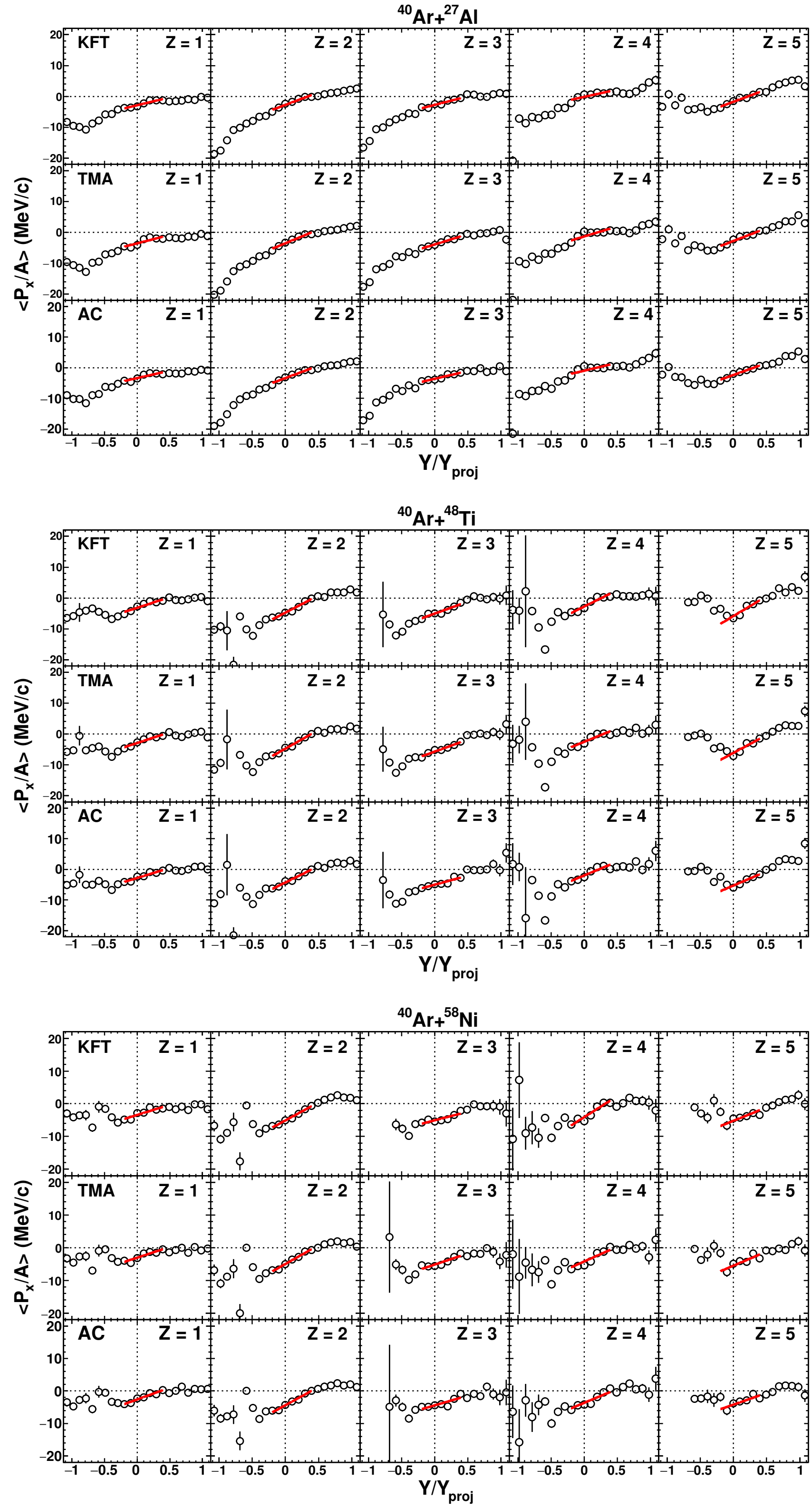

Figure 2: (Color online) Average in-plane momentum per nucleon $\langle P_x/A\rangle$ as a function of the scaled rapidity Y/Y_{proj} for $Z = 1-5$ fragments from the ^{40}Ar+^{27}Al, ^{40}Ar+^{48}Ti and ^{40}Ar+^{58}Ni reaction systems. Top, middle and bottom panels in each subfigure are the results from the reaction planes reconstructed using the KFT, TMA and AC methods as indicated on the left panels. Solid lines represent the linear fits for the data in the region of $-0.2 \leq Y/Y_{proj} \leq 0.4$.

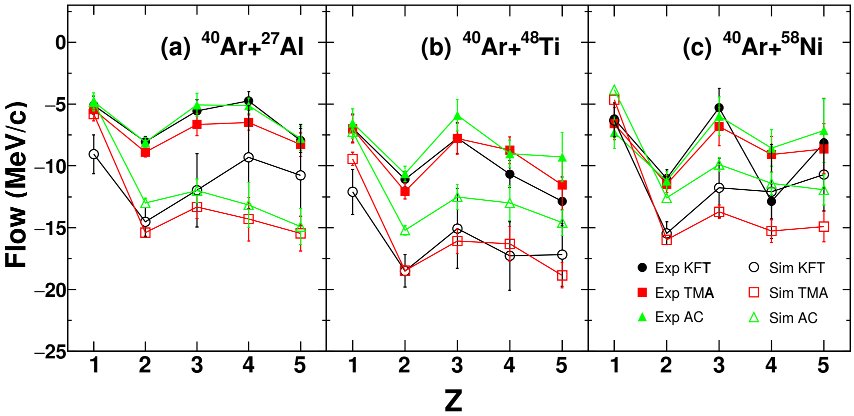

Figure 3: (Color online) Flow as a function of Z from (a) ^{40}Ar+^{27}Al, (b) ^{40}Ar+^{48}Ti and (c) ^{40}Ar+^{58}Ni. Solid dots, squares and triangles represent the experimental results obtained from the reaction planes reconstructed using the KFT, TMA and AC methods, respectively, whereas those from the filtered AMD-FM+Gemini events are correspondingly shown by circles, open squares and open triangles.

dicular squared distance between that line and the momentum position of each particle in the $x-y$ plane such that

$$D^2 = \sum_{\nu \neq POI} \left[P_x(\nu)^2 + P_y(\nu)^2 - \frac{[P_x(\nu) + kP_y(\nu)]^2}{1+k^2} \right]. \tag{4}$$

In Eq. (4), the POI is excluded from the summation over the fragments to avoid the autocorrelation [17], similar to the case of the TMA method. Differing from the KFT and TMA methods, the AC method is not able to provide the positive direction of the in-plane x-axis [17]. An additional technique must be used to determine the in-plane x-axis positive direction. In this work, the TMA method is applied as a supplemental method for the AC method following Ref. [17], permitting the consistency for reconstructing the reaction plane per particle.

The PFP method makes the use of only the kinematic information of projectile-like fragments. As demonstrated in Refs. [10, 29], the particles emitted from the excited projectile-like fragment may carry out-of-plane momenta which make the detected projectile-like fragment azimuthal direction different from the primary reaction plane, resulting in a poor reaction plane reconstruction. As the focus of this work is on accuracy of the reaction plane reconstruction, the PFP method is not used in this work, and all the other three, KFT, TMA and AC methods, explicitly taking into account the autocorrelation effect in the reaction plane reconstruction procedures, are applied in the following flow deduction from the in-plane components of fragment transverse momenta.

3. Results and discussion

a. Transverse flow deduced from in-plane components of fragment transverse momenta and experimental observation of abnormal α flow behavior

Transverse flow can be quantified from the in-plane transverse momenta using two equivalent definitions in general, i.e., slope flow [2, 3] and average in-plane transverse momentum flow [31]. Having the knowledge that both definitions are applicable for the absolute flow magnitude measurement, we adopt the definition of the slope for this work. For a certain type of fragments with mass number A, the transverse flow is calculated as [2, 3],

$$\text{Flow} = \left. \frac{d\langle P_x/A \rangle}{dY} \right|_{Y=0}, \tag{5}$$

where P_x and Y are the in-plane transverse momentum and the rapidity in the center-of-mass frame, respectively. Y is given by

$$Y = \frac{1}{2} \ln \frac{E + c \cdot P_z}{E - c \cdot P_z}, \tag{6}$$

where E and P_z are, respectively, the total energy and the longitudinal momentum in the center-of-mass frame. c is the velocity of light. In the practical analysis, the rapidity is scaled by the center-of-mass rapidity of the projectile [32], so that the projectile has $Y/Y_{proj} = 1$ and the mid-rapidity region is around $Y/Y_{proj} = 0$ in the center-of-mass frame. Unlike the case of model simulations for which the reaction planes are initially set and known, the reconstruction of the reaction plane in an event-by-event basis is demanded as a key intermediate procedure for deducing the flow values from the experimental events.

Figure 2 shows the average in-plane momentum per nucleon $\langle P_x/A \rangle$ as a function of the scaled rapidity Y/Y_{proj} for $Z = 1-5$ fragments for the reaction systems of ^{40}Ar+^{27}Al, ^{40}Ar+^{48}Ti and ^{40}Ar+^{58}Ni from the top to the bottom, respectively. The results with the $\langle P_x/A \rangle$ values evaluated in the reaction planes reconstructed using the KFT, TMA and AC methods are shown in the top, middle and bottom rows of each subfigure. The solid lines in the figure represent the linear fits to the data in the mid-rapiditiy region of $-0.2 \leq Y/Y_{proj} \leq 0.4$. Positive flow values are obtained from all the fits. The positive transverse flow values obtained are due to the application of the three reaction plane reconstruction methods [2, 3]. Since negative flow is expected due to the dominance of attractive mean field interaction at the present incident energy of 47 MeV/nucleon below the balance energy [9], negative signs are added in front of the

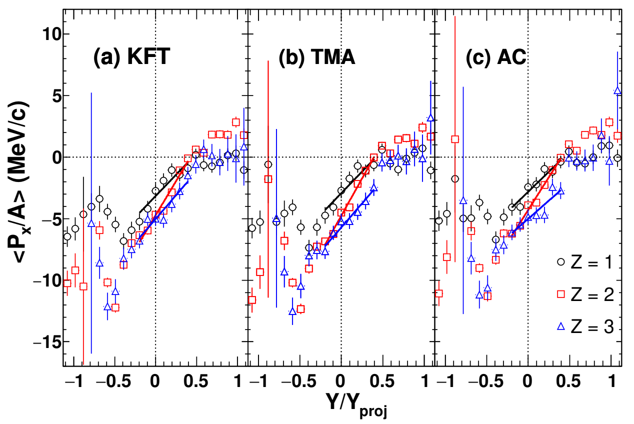

Figure 4: (Color online) Comparison of linear fits to average in-plane momentum per nucleon $\langle P_x/A \rangle$ as a function of the scaled rapidity Y/Y_{proj} for Z = 1−3 fragments from the ^{40}Ar+^{48}Ti system. The results are same as those of Fig. 2, but shown in an expanded scale along the Y-axis. Left, middle and right panels are those deduced using the KFT, TMA and AC methods, respectively.

extracted flow values. The obtained negative flow values are plotted as a function of Z in Fig. 3(a)-(c) for the three systems. Dots, squares and triangles in each panel represent the results obtained from the reaction planes reconstructed using the KFT, TMA and AC methods, respectively. The error bars shown are from the linear fits.

Most strikingly, rather good agreements, independent of the reaction systems, are observed for the transverse flow trends obtained using all the three reaction plane reconstruction methods. That is, using the KFT, TMA and AC methods for the three systems, the obtained flow trends all show non-monotonic increase as a function of Z with an abnormal α flow enhancement consistently. This consistency is clearly demonstrated in Fig. 4, in which the fits for the KFT, TMA and AC methods are compared in an expanded scale along the $\langle P_x/A \rangle$-axis, taking the results for Z=1,2,3 fragments from ^{40}Ar+^{48}Ti as an example. For all the three methods, the fitting slopes for Z=1 and 3 fragments are very similar to each other, whereas that for α particles shows significantly steeper. Our present results are in close agreement with the previous observations of the abnormal α behavior in Refs. [9, 10], where either the TMA method or the AC method was used for reconstructing the reaction planes as well. The consistency both in mass-dependent pattern and in flow magnitude for all the three reaction plane reconstruction methods, holding for all the three reaction systems, confirms the existence of the experimentally obtained abnormal α flow behavior following the present flow extraction procedures.

b. Inference for whether abnormal α flow behavior physically exists using AMD-FM simulations

In this subsection, an improved antisymmetrized molecular dynamics model in which the Fermi motion in the NN collision process has been taken into account explicitly, AMD-FM [13], is applied to investigate the physical existence of the abnormal α flow behavior. The selection of the AMD-FM is due to its success in describing both energy spectra and angular distributions of LCPs from heavy-ion collisions at intermediate energies [11, 13, 33], which is crucial for the present flow analysis. Around 150,000 events for ^{40}Ar+^{27}Al, ^{40}Ar+^{48}Ti and ^{40}Ar+^{58}Ni at 47 MeV/nucleon are simulated, respectively. The impact parameter for the simulations is adopted in the range of b/b_{max}=0.3-0.7 to maintain the consistency with those of the experimental analysis. The Gogny interaction [34] for the effective NN interaction and the in-medium cross sections of Li and Machleidt [35] are used for the NN collisions. The time evolution of the wave packets is computed up to 300 fm/c, and primary hot fragments at 300 fm/c are recognized using a coalescence technique with a coalescence radius of 5.0 fm in coordinate space. When the simulated results are compared with those of the experiment, the Gemini code [36] is used to statistically de-excite the hot fragments same as our previous work [33]. The primary events directly from the AMD-FM and those incorporating Gemini are denoted as the AMD-FM events and the AMD-FM+Gemini events hereinafter, respectively. To make direct comparison with the experimental data, the AMD-FM+Gemini events are further filtered using a software replica of the NIMROD-ISiS array.

The flow values for Z=1-5 fragments are extracted from the filtered AMD-FM+Gemini events using the same analysis procedure as the experimental data, and are compared with them in Fig. 3, where the former are presented by open symbols. Overall good agreements in the mass-dependent trend and magnitude are achieved between the flow values from the experiment and the filtered AMD-FM+Gemini events, though some slight deviations are observed beyond the error bars. These results demonstrate that the AMD-FM+Gemini simulations with a proper consideration of the NIMROD-ISiS filter are capable of reproducing the experimentally obtained flow mass-dependent trend reasonably well. Therefore, it is obvious to ask whether any abnormality of the α flow is suggested by the initial AMD-FM events.

In Fig. 5, the initial flow values are plotted by dots as a function of Z for the system of ^{40}Ar+^{48}Ti as a typical example, where they are extracted simply using the in-plane fragment momenta without using any reaction plane reconstruction methods. One may clearly observe that the initial flow shows a monotonic increase in the negative direction as mass increases without α flow enhancement. The same absence of the abnormal α flow behavior is also found in the other two systems. In one of our previous works [11], similar absence of the abnormal α flow behavior was also observed in the collisions of ^{40}Ca+ ^{40}Ca at 35 MeV/nucleon simulated by the AMD-FM and the constrained molecular dynamics (CoMD) model [37]. For comparison, the extracted flow values from the AMD-FM events with the three reaction plane reconstruction methods are plotted in the figure. All these results show essentially the same flow characteristics with pronounced abnormal α flow enhancement as those derived from the experimental data, once the procedure of reaction plane reconstruction is involved in the flow extraction. The dependence of the α flow enhancement upon the application of reaction plane reconstruction method here strongly suggests that the experimentally observed “abnormal” α flow

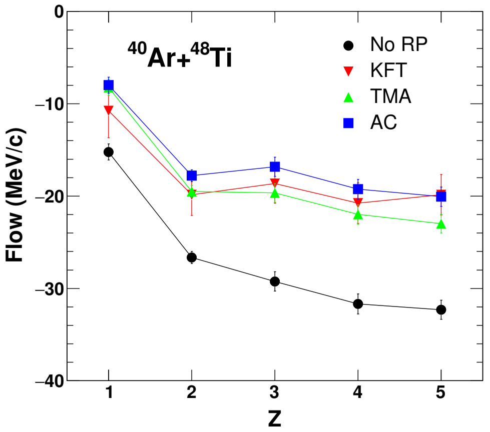

Figure 5: (Color online) Flow as a function of Z from the AMD-FM events of ^{40}Ar+^{48}Ti. Dots are the results deduced without the reaction plane reconstruction process (No RP), and inverted triangles, triangles, and squares are those from the reaction planes reconstructed using the KFT, TMA and AC methods, respectively.

behavior may not physically exist in nature. The overall underestimation of flow values after applying the three methods for reconstructing the reaction plane means that none of the methods provides the reaction plane accurately enough to extract the real flow values, revealing the weakness of the reaction plane reconstruction using current methods.

c. Investigation on physical existence of abnormal α flow behavior using reaction plane-free two-particle azimuthal correlation method

With the indication for the inexistence of the abnormal α flow behavior in nature from the above comparison of the present experimental mass dependent flow measurements and the AMD-FM simulations in mind, we continue to pursue the physical existence of abnormal α flow behavior using a two-particle azimuthal correlation (2pAC) method of Wang *et al.* [18]. The 2pAC method has been shown to provide potentially powerful probe for the flow generated in the heavy-ion collisions at energies from several ten MeV to several TeV [18, 38, 39, 40, 41]. Unlike conventional flow extraction methods discussed above, the flow extraction in the 2pAC method does not require the knowledge of the reaction plane, and as a consequence, it does not suffer from the uncertainties associated with the reaction plane reconstruction. Therefore, direct observation of whether the abnormal α flow behavior exists or not can be achieved eliminating the influence imposed by the reaction plane reconstruction procedure.

The 2pAC method was designed to make use of two-particle azimuthal correlation function. Following Refs. [18, 38], it is defined by a ratio of two distributions

$$C(\Delta\phi) = \frac{N_{cor}(\Delta\phi)}{N_{uncor}(\Delta\phi)}, \tag{7}$$

where $N_{cor}(\Delta\phi)$ in the numerator is the measured $\Delta\phi$ distribution for the correlated particle pairs from the same event, and $N_{uncor}(\Delta\phi)$ in the denominator is the $\Delta\phi$ distribution for uncorrelated particle pairs generated by the mixing of events such that each member of a pair is randomly selected from two different events. The $\Delta\phi$ angle is the angle between the transverse momenta of two correlated/uncorrelated particles in each given pair. For a given event, there are $M_f(M_f-1)/2$ correlated particle pairs, where M_f is the number of measured fragments, and thus $M_f(M_f-1)/2$ entries for $C(\Delta\phi)$ are obtained in one event. Detailed description about the $C(\Delta\phi)$ construction is referred to Refs. [18, 38].

Under the assumption of independent statistical emission of particles with the same azimuthal distribution $F(\phi)$ in an event, the azimuthal correlation function is simply related to $F(\phi)$ via the convolution [39, 42]

$$C(\Delta\phi) = \int_0^{2\pi} F(\phi)F(\phi+\Delta\phi)d\phi. \tag{8}$$

From previous studies [39, 43], we know the azimuthal distribution of emitted particles can be described well via the Legendre polynomial expansion up to the second order

$$F(\phi) = f_0[1 + f_1\cos(\phi) + f_2\cos(2\phi)]. \tag{9}$$

The coefficient f_1 is related to the anisotropic collective motion and its magnitude can reflect roughly the magnitude of the flow [43], i.e., the larger the absolute value of f_1 is, the stronger the in-plane flow is; the coefficient f_2 is related to the rotational collective motion which was focused on in other works [38, 39, 40]. The coefficient f_0 is a constant. Inserting Eq. (9) into Eq. (8), one can derive the form of $C(\Delta\phi)$ to be

$$C(\Delta\phi) = f_0^2[1 + 0.5f_1^2\cos(\Delta\phi) + 0.5f_2^2\cos(2\Delta\phi)]. \tag{10}$$

The in-plane flow information can be therefore extracted by optimizing f_1 from the fit to the experimentally constructed $C(\Delta\phi)$ using Eq. (10). Note that f_1 is different from the flow values from the in-plane components of fragment transverse momenta discussed in the above subsections. Here, f_1 is normalized by f_0 and dimensionless as defined in Eq. (9), whereas the flow in the above subsections is with a dimension of momentum. In spite of being not capable of reflecting the absolute flow magnitude, f_1 deduced using the 2pAC method reflects the relative flow magnitude, so that it is applicable for the present study on the mass dependent behavior of the flow. To distinguish from those quantified from the in-plane transverse momenta in the above subsections, we refer f_1 as the "relative" flow magnitude hereinafter.

As pointed out in Ref. [18], the Coulomb interaction and the effect of quantum statistics for identical particles affect the two-particle azimuthal correlation function, potentially influencing the relative flow magnitude determination. To minimize the two effects, the particle pairs with low relative momenta $|\Delta p|$ <50 MeV/c [18] are excluded from the obtained $N_{cor}(\Delta\phi)$ distribution. Another experimental limitation for constructing the $N_{cor}(\Delta\phi)$ one should consider seriously is that the two correlated particles tend to fly in the same direction, but only one of them can be detected if they hit the same detector

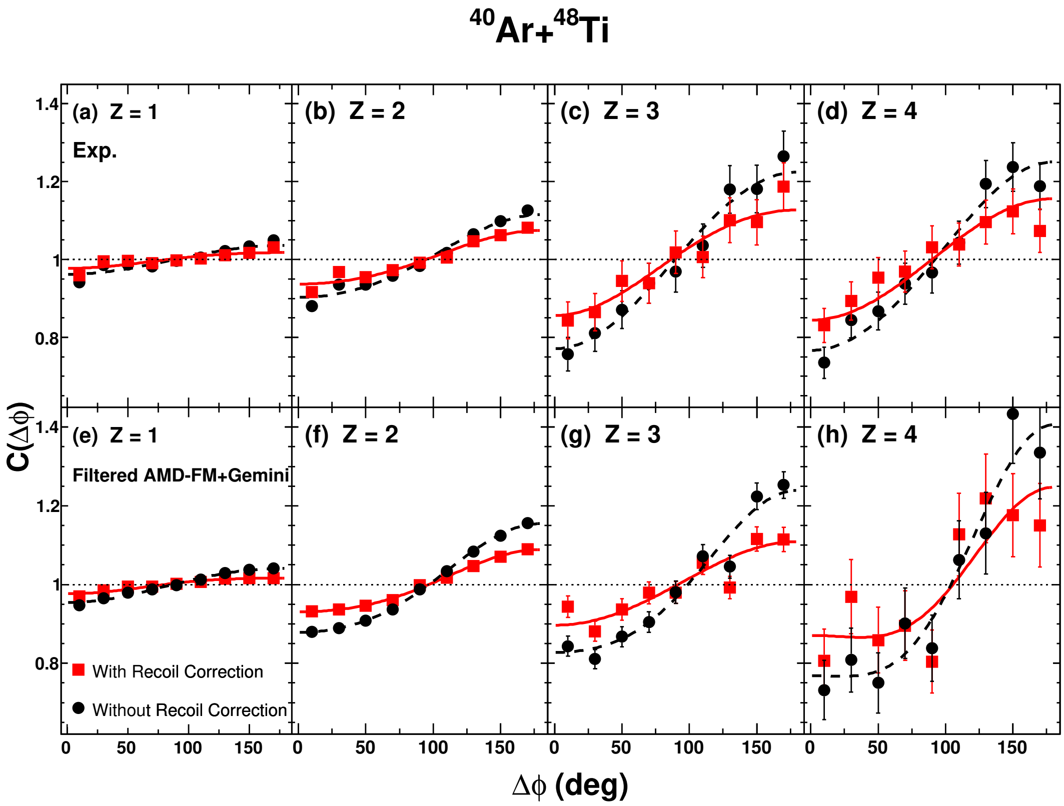

Figure 6: Two-particle azimuthal correlation functions $C(\Delta\phi)$ for $Z = 1-4$ pairs with (squares) and without (dots) the correction for the recoil effect from the system of ^{40}Ar+^{48}Ti. The results shown in (a)-(d) are obtained from the experimental data, whereas those shown in (e)-(h) are from the filtered AMD-FM+Gemini events. The Z number for labeling each panel corresponds to the $C(\Delta\phi)$ for which both correlated particles are demanded to be with the same given Z number in each of the pairs used to determine $\Delta\phi$. Solid and dashed curves in each panel represent the fits to the results with and without the correction for the recoil effect using Eq. (12).

in one event. This limitation results in large uncertainties in the $N_{cor}(\Delta\phi)$ construction. To solve this problem, the correlated particle pairs both with negative values of center-of-mass rapidity were only taken into account in the early work of Lacey *et al.* [38], taking the advantage of relatively better angular resolutions of the detector modules in the backward center-of-mass hemisphere. This selection is effective, but results in a significant loss of statistics due to the larger detector energy thresholds in the backward at the same time. For this work, to make an improvement, we demand the correlated particle pairs with different rapidity signs in the center-of-mass frame, allowing to take into account the detector angular resolutions and energy thresholds simultaneously.

Since the reaction systems used for our present study are small, the momentum conservation effect is also expected to have a pronounced effect on the two-particle azimuthal correlation function. Indeed, it has been pointed out in the previous studies of Chitwood *et al.* [44] and Prendergast *et al.* [45] that the momentum conservation effect significantly affects the shape of the azimuthal correlation function in small reaction systems. Therefore, correction for the momentum conservation effect is further required prior to deducing the relative flow magnitude from the two-particle azimuthal correlation function. Here, we adopt the approximate treatment for considering the momentum conservation effect in the single static-source model previously used to pursue the origin of the azimuthal correlation function deformation in Refs. [45, 44]. In the center-of-mass frame, for the two correlated particles with mass numbers A_1 and A_2, and center-of-mass transverse velocities $\vec{v_1}$ and $\vec{v_2}$, they are assumed to be emitted from a single source with mass number A_0 and initial center-of-mass transverse velocity zero sequentially. After the emission of the first particle from the source, the residue with mass number $A_0 - A_1$ gains additional transverse velocity $\Delta\vec{v_r}$ due to the recoil by the momentum conservation,

$$\Delta\vec{v_r} = -\frac{A_1}{A_0 - A_1}\vec{v_1}. \tag{11}$$

For the emission of the second particle from the residue, the additional transverse velocity, which is from the recoil of the first particle but nothing to do with the collective motion, is inherited as a consequence. Following this scenario, one is able to experimentally handle the correction for the recoil due to the momentum conservation by adding $-\Delta\vec{v_r}$ to the measured transverse velocity of the second particle $\vec{v_2}$. Similar approach has been also applied to the correction for the recoil effect from the POIs in the reaction plane reconstruction [16].

Figure 6(a)-(d) shows the obtained two-particle azimuthal correlation functions $C(\Delta\phi)$ deduced from the same selected data set of the ^{40}Ar+^{48}Ti reaction used to produce Figs. 2 to 4 with the recoil correction with the identification of Z as an example (squares). The $C(\Delta\phi)$ labeled by Z in each panel corresponds to the result in which we demand both correlated particles to be with the same given Z number in each of the pairs used to determine $\Delta\phi$ (with no selection in isotope type). For example, the label "Z = 3" in Fig. 6(c) indicates that only the lithium-lithium pairs are taken to construct the $C(\Delta\phi)$ in that panel. Similar treatment was adopted in the previous work of by Prendergast *et al.* [45] and elsewhere. The errors shown for the data points are of statistical origin in each case. It should be mentioned that the $C(\Delta\phi)$ from boron-boron pairs is absent from the figure due to the statistics. However as found below, the results from $Z = 1-4$ pairs are enough to conduct the following discussion. In Fig. 6(a)-(d), the $C(\Delta\phi)$ shows remarkable azimuthal asymmetries for all $Z = 1-4$ pairs being with the magnitudes more than unity at $\Delta\phi = 180°$ and less than unity at $\Delta\phi = 0°$. One may notice that our results show the peak position at $\Delta\phi = 180°$ rather than at $\Delta\phi = 0°$, in contrast to those of Wang *et al.* [18] and Lacey *et al.* [38] etc. This can be attributed to the fact that the in-plane anisotropic collective motion causes the two correlated particles to move in a back-to-back configuration, for the present correlated particle pairs for which the condition of being with different rapidity signs in the center-of-mass frame is demanded.

Under this condition, the two correlated particles have symmetric azimuthal distributions such as $F(\Delta\phi)$ and $F(\Delta\phi+180°)$, rather than having the same azimuthal distribution $F(\Delta\phi)$ as assumed in Eq. (8). Following the same derivation from Eq. (8) to Eq. (10), one can find Eq. (10) changes to

$$C(\Delta\phi) = f_0^2[1 - 0.5f_1^2\cos(\Delta\phi) + 0.5f_2^2\cos(2\Delta\phi)], \qquad (12)$$

for the present work. To extract the relative flow values from the obtained $C(\Delta\phi)$, we perform the fits to the $C(\Delta\phi)$ distributions using Eq. (12) with the coefficient f_0 being equal to 1 based on the previous work of Lacey *et al.* [38]. The best fits to the data are shown by solid curves in Fig. 6(a)-(d). The obtained relative flow values f_1 for the $Z = 1-4$ pairs are plotted as a function of Z by squares in Fig. 7(a). The errors are from the fits. Here, negative signs are taken for f_1 due to the dominance of the attractive mean field interaction at the present incident energy of 47 MeV/nucleon, similar to the case of Fig. 2. Clearly, the obtained f_1 values with the correction for the momentum conservation increase monotonically in the negative direction as Z increases, showing no abnormal α flow enhancement. The same absence of the abnormal α flow behavior is also found in the other two systems. This result, in addition to the indication found from the comparison in the above subsection using the AMD-FM, definitely provides a direct experimental evidence for the inexistence of the abnormal α flow behavior in nature.

To provide deeper insight into the influence of the momentum conservation on the f_1, the $C(\Delta\phi)$ distributions without the correction for the recoil effect are shown by dots in Fig. 6(a)-(d) for comparison. The $C(\Delta\phi)$ distributions without the recoil correction show more remarkable azimuthal asymmetries compared to those with the recoil correction systematically, indicating a significant modification of $C(\Delta\phi)$ due to the recoil effect imposed by the momentum conservation. We fit the $C(\Delta\phi)$ using Eq. (12) (dashed curves), and plot the extracted f_1 values as a function of Z by dots in Fig. 7(a). In the figure, the obtained f_1 values show a monotonic trend as Z increases as well, similar to that with the recoil correction. In contrast, the f_1 values without the recoil correction are overall larger than those with the recoil correction, and their deviations increase from ~0.1 to ~0.2 as Z increases from 1 to 4. The f_1 value enhancement after turning off the recoil correction can be interpreted that the recoil from the momentum conservation drives the two correlated particles to move in a back-to-back configuration, being with the same function of the in-plane anisotropic collective motion under the present condition of the correlated particle pair selection. Therefore, the recoil effect enlarges the f_1 values by superimposing onto the in-plane anisotropic collective motion. As the recoil effect is more significant for heavier fragments, larger f_1 enhancment is found for the heavier correlated particle pairs after turning off the recoil correction. The comparison in Fig. 7(a) suggests that whether the recoil effect is corrected or not only weakly jeopardizes the mass-dependent trend of f_1, but the f_1 magnitude strongly depends upon the application of correction for the recoil effect. We also re-extract the flow values which have been given in Figs. 3 and 5 with the correction

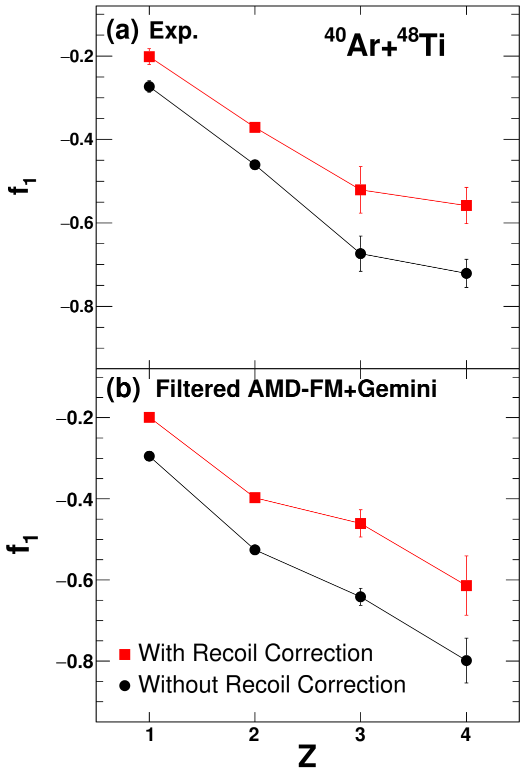

Figure 7: Relative flow magnitude f_1 as a function of Z extracted from the $C(\Delta\phi)$ with (squares) and without (dots) the recoil effect correction from the collision system of ^{40}Ar+^{48}Ti. The results shown in (a) are obtained from the experimental data, whereas those shown in (b) are from the filtered AMD-FM+Gemini events.

for the recoil effect from the POIs in the reaction plane reconstruction using the correction method in the present 2pAC analysis for cross-checking. The results consistently indicate that, although the absolute flow values slightly decrease as well, the conclusions related to the flow mass-dependent behavior drawn in Sec. 3(a) and (b) are fully valid.

For completeness, we perform the same 2pAC analysis using the filtered AMD-FM+Gemini events which have been used in Fig. 3 (see details about the AMD-FM calculations and the filter inclusion in Sec. 3(b)). The $C(\Delta\phi)$ and f_1 results are plotted together with those of experiment in Fig. 6(e)-(h) and Fig. 7(b), respectively. From the comparisons between Fig. 6(a)-(d) and (e)-(h), close agreements are clearly found for the $C(\Delta\phi)$ results from the experiment and the filtered AMD-FM+Gemini events. In Fig. 7(b), the deduced f_1 values from the filtered AMD-FM+Gemini events also show no abnormal α flow behaviors, similar to those of the experiment shown in Fig. 7(a), in spite of being with slight deviations in magnitude. The reasonable reproductions of the experimental results both in $C(\Delta\phi)$ and in f_1 by the AMD-FM simulations provide sufficient theoretical support to the correction for the recoil effect and the conclusion drawn from the present 2pAC analysis.

It is worth emphasizing again that the presently applied 2pAC method can only provide a probe of the relative flow magnitude, rather than the absolute flow magnitude. There are some other powerful methods, i.e., the transverse momentum analysis technique proposed by Danielewicz *et al.* [19, 46] etc, being capable of deducing the absolute flow values without the reaction plane reconstruction. It will be of great importance to further investigate the issues related to the transverse flow using these reaction plane-free methods in future.

4. Summary and prospectives

In summary, transverse flow values for Z=1-5 fragments from the collisions of ^{40}Ar+^{27}Al, ^{40}Ar+^{48}Ti and ^{40}Ar+^{58}Ni at 47 MeV/nucleon have been determined using the in-plane transverse momentum components of the fragments. It is found that the experimentally obtained flow values deduced with the application of the conventional methods, i.e., the KFT, TMA and AC methods with the consideration of the autocorrelation effect, for reconstructing the reaction plane show an abnormal α flow enhancement as the fragment mass increases. The close comparison between the experimental results and those from the AMD-FM simulations suggests that the abnormal α behavior is not real, but originates from the inaccurate reconstruction of the reaction plane using the KFT, TMA and AC methods. Further, the 2pAC method, which allows to deduce the relative flow magnitude without the knowledge of the reaction plane, is applied to investigate the physical existence of abnormal α flow behavior. The obtained relative flow magnitudes deduced from the two-particle azimuthal correlation functions with an identification of Z, with consideration for the recoil effect imposed by the momentum conservation, increase monotonically in the negative direction as Z increases, definitely leading to a conclusion that the abnormal α transverse flow enhancement does not exist in the actual heavy-ion collisions at the present incident energy region in nature.

As a final remark, the present work also reveals the problem of inaccuracies in the reaction plane reconstruction which was widely acknowledged 20-30 years ago, but has been neglected nowadays. More efforts for improving the accuracy of the current reaction plane reconstruction methods or developing novel methods with high accuracy are still urgently required at present. Recently, artificial intelligence has been introduced to determine the heavy-ion collision centrality in nuclear physics, and better performance is achieved comparing to using the traditional methods [47]. Making use of the capacity of recognizing and characterizing complex data sets of the artificial intelligence techniques may help to better determine reaction planes in heavy-ion collisions in future.

5. Acknowledgments

The authors thank the operational staff in the Cyclotron Institute, Texas A&M University, for their support during the experiment and for the fruitful discussion. This work is supported by the National Natural Science Foundation of China (No. 11705242, U1632138, 11805138, 11905120, 11975091, 11947416), the Fundamental Research Funds For the Central Universities (No. YJ201954 and YJ201820) in China, and International Visiting Program for Excellent Young Scholars of Sichuan University. This work is also supported by the US Department of Energy under 376 Grant No. DE-FG02-93ER40773 and the Robert A. Welch Foundation under Grant A330.

[1] P. Danielewicz, R. Lacey and W.G. Lynch, Sci. **298**, 1592 (2002).
[2] R. Pak, W. Benenson, O. Bjarki, J. A. Brown, S. A. Hannuschke, R. A. Lacey, Bao-An Li, A. Nadasen, E. Norbeck, P. Pogodin, D. E. Russ, M. Steiner *et al.*, Phys. Rev. Lett. **78**, 1022 (1997).
[3] R. Pak, Bao-An Li, W. Benenson, O. Bjarki, J. A. Brown, S. A. Hannuschke, R. A. Lacey, D. J. Magestro, A. Nadasen, E. Norbeck, D. E. Russ, M. Steiner *et al.*, Phys. Rev. Lett. **78**, 1026 (1997).
[4] Z. Kohley, L. W. May, S. Wuenschel, A. Bonasera, K. Hagel, R. Tripathi, R. Wada, G. A. Souliotis, D. V. Shetty, S. Galanopoulos, M. Mehlman, W. B. Smith *et al.*, Phys. Rev. **C 82**, 064601 (2010).
[5] Z. Kohley, L. W. May, S. Wuenschel, M. Colonna, M. Di Toro, M. Zielinska-Pfabé, K. Hagel, R. Tripathi, A. Bonasera, G. A. Souliotis, D. V. Shetty, S. Galanopoulos *et al.*, Phys. Rev. **C 83**, 044601 (2011).
[6] Z. Kohley, M. Colonna, A. Bonasera, L. W. May, S. Wuenschel, M. Di Toro, S. Galanopoulos, K. Hagel, M. Mehlman, W. B. Smith, G. A. Souliotis, S. N. Soisson *et al.*, Phys. Rev. **C 85**, 064605 (2012).
[7] A. Ono and H. Horiuchi, Phys. Rev. **C 51**, 299 (1995).
[8] M. J. Huang, R. C. Lemmon, F. Daffin, W. G. Lynch, C. Schwarz, M. B. Tsang, C. Williams, P. Danielewicz, K. Haglin, W. Bauer, N. Carlin, R. J. Charity *et al.*, Phys. Rev. Lett. **77**, 3739 (1996).
[9] D. Cussol, T. Lefort, J. Péter, G. Auger, Ch. O. Bacri, F. Bocage, B. Borderie, R. Bougault, R. Brou, Ph. Buchet, J. L. Charvet, A. Chbihi *et al.*, Phys. Rev. **C 65**, 044604 (2002).
[10] X. Liu, W. Lin, R. Wada, M. Huang, Z. Chen, G. Q. Xiao, S. Zhang, R. Han, M. H. Zhao, P. Ren, Z. Jin, J. Liu, F. Shi, J. B. Natowitz *et al.*, Phys. Rev. **C 90**, 014604 (2014).
[11] G. Qu, Y. Huang, D. Peng, Z. Xu, W. Lin, H. Zheng, G. Tian, R. Han, C. Ma, M. Huang, P. Ren, J. Han *et al.*, Phys. Rev. **C 103**, 044607 (2021).
[12] A. Ono and H. Horiuchi, Prog. in Part. and Nucl. Phys. **53**, 501-581(2004).
[13] W. Lin, X. Liu, R. Wada, M. Huang, P. Ren, G. Tian, F. Luo, Q. Sun, Z. Chen, G. Q. Xiao, R. Han, F. Shi *et al.*, Phys. Rev. **C 94**, 064609 (2016).
[14] J. Cugnon and D. L'Hote, Nucl. Phys. **A 397**, 519 (1983).

[15] P. Danielewicz and G. Odyniec, Phys. Lett. **B 157**, 146 (1985).
[16] C. A. Ogilvie, D. A. Cebra, J. Clayton, P. Danielewicz, S. Howden, J. Karn, A. Nadasen, A. Vander Molen, G. D. Westfall, W. K. Wilson, and J. S. Winfield, Phys. Rev. **C 40**, 2592 (1989).
[17] W. K. Wilson, R. Lacey, C. A. Ogilvie, and G. D. Westfall, Phys. Rev. **C 45**, 738 (1992).
[18] S. Wang, Y. Z. Jiang, Y. M. Liu, D. Keane, D. Beavis, S. Y. Chu, S. Y. Fung, M. Vient, C. Hartnack and H. Stöcker, Phys. Rev. **C 44**, 1091 (1991).
[19] P. Danielewicz, H. Ströbele, G. Odyniec, D. Bangert, R. Bock, R. Brockmann, J. W. Harris, H. G. Pugh, W. Rauch, R. E. Renfordt, A. Sandoval, D. Schall, L. S. Schroeder, and R. Stock, Phys. Rev. C 38, 120 (1988).
[20] S. Wuenschel, K. Hagel, R. Wada, J. B. Natowitz, S. J. Yennello, Z. Kohley, C. Bottosso, L. W. May, W. B. Smith, D. V. Shetty, B. C. Stein, S. N. Soisson, G. Prete, Nucl. Instrum. Methods Phys. Res., Sect. **A 604**, 578 (2009).
[21] R. P. Schmitt, L. Cooke, G. Derrig, D. Fabris, B. Hurst, J. B. Natowitz, G. Nebbia, D. O'Kelly, B. K. Srivastava, W. Turmel, D. Utley, H. Utsunomiya and R. Wada, Nucl. Instrum. Methods Phys. Res., Sect. **A 354**, 487 (1995).
[22] Y. G. Ma, J. B. Natowitz, R. Wada, K. Hagel, J. Wang, T. Keutgen, Z. Majka, M. Murray, L. Qin, P. Smith, R. Alfaro, J. Cibor, M. Cinausero, Y. El Masri, D. Fabris, E. Fioretto, A. Keksis, M. Lunardon, A. Makeev *et al.*, Phys. Rev. **C 71**, 054606 (2005).
[23] R. Wada, W. Lin, P. Ren, H. Zheng, X. Liu, M. Huang, K. Yang, and K. Hagel, Phys. Rev. **C 99**, 024616 (2019).
[24] L. Phair, D. R. Bowman, C. K. Gelbke, W. G. Gong, Y. D. Kim, M. A. Lisa, W. G. Lynch, G. F. Peaslee, R. T. de Souza, M. B. Tsang and F. Zhu, Nucl. Phys. **A 548**, 489 (1992).
[25] F. Zhu, W. G. Lynch, D. R. Bowman, R. T. de Souza, C. K. Gelbke, Y. D. Kim, L. Phair, M. B. Tsang, C. Williams, and H. M. Xu, Phys. Rev. **C 52**, 784 (1995).
[26] M. Di Toro, S. J. Yennello, and Bao-An Li, Eur. Phys. J. **A 30**, 153 (2006).
[27] R. Pak, W. J. Llope, D. Craig, E. E. Gualtieri, S. A. Hannuschke, R. A. Lacey, J. Lauret, A. C. Mignerey, D. E. Russ, N. T. B. Stone, A. M. Vander Molen, G. D. Westfall, and J. Yee, Phys. Rev. **C 53**, R1469 (1996).
[28] Z. Kohley, A. Bonasera, S. Galanopoulos, K. Hagel, L. W. May, A. B. McIntosh, B. C. Stein, G. A. Souliotis, R. Tripathi, S. Wuenschel, and S. J. Yennello, Phys. Rev. **C 86**, 044605 (2012).
[29] W. Q. Shen, J. Péter, G. Bizard, R. Brou, D. Cussol, M. Louvel, J. P. Patry, R. Régimbart, J. C. Steckmeyer, J. P. Sullivana, B. Tamain, E. Crema, H. Doubre, K. Hagel *et al.*, Nucl. Phys. **A 551**, 333 (1993).
[30] J. C. Angélique, A. Buta, G. Bizard, D.Cussol, A. Péghaire, J. Péter, R. Popescu, G. Auger, R. Brou, C. Cabot, E. Crema, Y. El Masri, P. Eudes, Z. Y . He, A. Kerambrun, C. Lebrun, R. Regimbart *et al.*, Nucl. Phys. **A 614**, 261 (1997).
[31] A. Bonasera, F. Gulminelli, and J. Molitoris, Phys. Rep. **243**, 1 (1994).
[32] A. Bonasera and L. P. Csernai, Phys. Rev. Lett. **59**, 630 (1987).
[33] G. Tian, R. Wada, Z. Chen, R. Han, W. Lin, X. Liu, P. Ren, F. Shi, F. Luo, Q. Sun, L. Song, and G. Q. Xiao, Phys. Rev. **C 95**, 044613 (2017).
[34] A. Ono, H. Horiuchi, Toshiki Maruyama, and A. Ohnishi, Prog. Theor. Phys. **87**, 1185 (1992).
[35] G. Q. Li and R. Machleidt, Phys. Rev. **C 48**, 1702 (1993) and Phys. Rev. **49**, 566 (1994).
[36] R. J. Charity, M. A. Mcmahan, G. J. Wozniak, R. J. Mcdonald, L. G. Moretto, D. G. Sarantites, L. G. Sobotka, G. Guarino, A. Pantaleo, L. Fiore, A. Gobbi, K. D. Hildenrand, Nucl. Phys. **A 483**, 371 (1988).
[37] M. Papa, G. Giuliani, and A. Bonasera, J. Comput. Phys. **208**, 403 (2005).
[38] Roy A. Lacey, A. Elmaani, J. Lauret, T. Li, W. Bauer, D. Craig, M. Cronqvist, E. Gualtieri, S. Hannuschke, T. Reposeur, A. Vander Molen, G. D. Westfall, W. K. Wilson, J. S. Winfield, J. Yee, S. Yennello, A. Nadasen, R. S. Tickle, and E. Norbeck, Phys. Rev. Lett. **70**, 1224 (1993).
[39] Y. G. Ma and W. Q. Shen, Phys. Rev. **C 51**, 3256 (1995).
[40] G. Singh and P. L. Jain, Phys. Rev. **C 49**, 3320 (1994).
[41] M. Dordevic, J. Milosevic, L. Nadderd, M. Stojanovic, F. Wang, and X. Zhu, Phys. Rev. **C 101**, 014908 (2020).
[42] M. B. Tsang, P. Danielewicz, D. R. Bowman, N. Carlin, R. T. de Souza, C. K. Gelbke, W. G. Gong, Y. D. Kim, W. G. Lynch, L. Phair, and F. Zhu, Phys. Lett. **B 297**, 243 (1992).
[43] Y. G. Ma, W. Q. Shen, J. Feng, and Y. Q. Ma, Phys. Rev. **C 48**, R1492 (1993).
[44] C. B. Chitwood, D. J. Fields, C. K. Gelbke, D. R. Klesch, W. G. Lynch, M. B. Tsang, T. C. Awes, R. L. Ferguson, F. E. Obenshain, F. Plasil, R. L. Robinson, and G. R. Young, Phys. Rev. **C 34**, 858 (1986).
[45] E. P. Prendergast, A. van den Brink, A. P. de Haas, R. Kamermans, P. G. Kuijer, C. T. A. M. de Laat, R. W. Ostendorf, E. Oti, A. Péghaire, and R. J. M. Snellings, Phys. Rev. **C 61**, 024611 (2000).
[46] M. B. Tsang, P. Danielewicz, W. C. Hsi, M. Huang, W. G. Lynch, D. R. Bowman, C. K. Gelbke, M. A. Lisa, G. F. Peaslee, R. J. Charity, L. G. Sobotka *et al.*, Phys. Rev. **C 53**, 1959 (1996).
[47] F. Li, Y. Wang, H. Lü, P. Li, Q. Li and F. Liu, J. Phys. G: Nucl. Part. Phys. **47**, 115104 (2020).